GeoConvention
Calgary • Canada • March 7-11 2016
OPTIMIZING RESOURCES

Mitigate Cycle-skipping for Full-waveform Inversion by Band-limited Impedance Inversion and POCS

Wenyong Pan, Kris Innanen, Gary Margrave and Scott Keating
CREWES Project, Department of Geoscience, University of Calgary

Summary

Full-waveform inversion (FWI) promises to provide high-resolution estimates of subsurface parameters. While, FWI suffers from the cycle-skipping difficulty arising from the lack of low frequency information and inaccurate initial model. In this paper, we aim at recovering low frequency information by band-limited impedance inversion from well data combining with project onto convex sets (POCS) algorithm. The low frequency components in the reflectivity section are recovered by POCS algorithm. A band-limited impedance inversion is then performed with the interpolated well log model. Through this process, an enhanced initial model is built for mitigate the cycle-skipping problem in FWI.

Introduction

Full-waveform inversion (FWI) allows to reconstruct high-resolution velocity models of the subsurface through the extraction of the full information content of the seismic data data (Lailly, 1983; Tarantola, 1984; Virieux and Operto, 2009). FWI iteratively minimizes a L-2 norm misfit function, which measures the difference between the modelled data and observed data (Pratt et al., 1998; Pan et al., 2014b, 2015a, 2015b).

FWI is promising but also suffers from a lot challenges, one of which is the cycle-skipping difficulty. The inversion process is classically solved with local optimization schemes and is therefore strongly dependent on the starting model definition. One key assumption and criteria in the localized inversion is that the modelled and observed waveforms are within half a wave-cycle at the lowest frequency to converge iteratively in the right direction. Theoretically, at low frequencies, there is a high chance that the modelled and observed data match within half a wave-cycle. Hence, the low frequencies are crucial to recover the long wavelength structures of the model.

However, in traditional seismic data, the low frequencies are missed, which results in that FWI applications are always trapped in local minimum. Impedance inversion is very useful for reservoir characterization and band-limited impedance inversion (BLIMP) is implemented by incorporating low frequency information from well log data. In this paper, we consider recovering the low frequencies from well log data for full-waveform inversion through the band-limited impedance inversion. The impedance inversion result is used as the initial model for full-waveform inversion. However, one problem is that the traces far away from the well log positions may not be reliable. In this paper, we are also trying to recover the low frequencies for the reflectivity section using a projection onto convex sets (POCS) algorithm. POCS algorithm is generally employed to infill missing seismic data in seismic data reconstruction. In this paper, we attempt to use this method to recover the low frequencies, based on a series of assumptions (Innanen, 2011).

The paper is organized as follows. We first review the basic principle of non-linear least-squares inverse problem. Then, we introduce the POCS algorithm and the band-limited impedance inversion method. The proposed strategies which combine band-limited impedance inversion and POCS algorithm is explained. In

the numerical section, we first illustrate with numerical examples the effects of cycle-skipping in FWI. Then, we show the effectiveness of the proposed strategies in mitigating cycle-skipping problem.

Review of non-linear least-squares inverse problem

As a non-linear least-squares optimization problem, FWI seeks to estimate the subsurface parameters by iteratively minimizing the difference between the synthetic data and observed data. The misfit function is formulated in a least-squares form:

$$\Phi(\mathbf{m}) = \frac{1}{2}\sum_{\mathbf{x}_s}\sum_{\mathbf{x}_r}\sum_{\omega}\left\|\Delta\mathbf{d}(\mathbf{x}_r,\mathbf{x}_s,\omega)\right\|^2, \tag{1}$$

where $\mathbf{x}_r$ and $\mathbf{x}_s$ indicate the locations of receivers and sources, $\Delta\mathbf{d}$ is the data residual vector and ω is the angular frequency. To minimize the quadratic approximation of the misfit function, the updated model at k+1 iteration can be written as the sum of the model at the kth iteration and the search direction:

$$\mathbf{m}_{k+1} = \mathbf{m}_k + \mu_k \Delta\mathbf{m}_k, \tag{2}$$

where μ_k is the step length, a scalar constant calculated through a line search method satisfying the weak Wolfe condition. The gradient can be constructed by cross-correlating the forward modelled wavefield and back-propagated wavefield:

$$\mathbf{g(x)}=\sum_{\omega}\sum_{\mathbf{x}_s}\sum_{\mathbf{x}_r}\sum_{\mathbf{x}_s^{'}}\Re(\omega^2 f_s(\omega)G(\mathbf{x},\mathbf{x}_s,\omega)G(\mathbf{x},\mathbf{x}_r,\omega)\Delta\mathbf{d}^*(\mathbf{x}_r,\mathbf{x}_s^{'},\omega)), \tag{3}$$

where $f_s(\omega)$ indicates the source signature, $G(\mathbf{x},\mathbf{x}_s,\omega)$ and $G(\mathbf{x},\mathbf{x}_r,\omega)$ are the source-side and receiver-side Green's functions respectively.

Projection onto convex sets (POCS) algorithm

The projection onto convex sets (POCS) algorithm is implemented in an iterative scheme (Innanen, 2011). We suppose that the measure trace $s_0(t)$ is deficient in frequencies below f_0. The threshold operator γ_0 is used to generate trace $y_0(t) = \gamma s_0(t)$. For trace $y_0(t)$, it is equal to $s_0(t)$ for all values above the threshold, and zero everywhere else. A new spectrum is generated, equal to $S_0(f)$ within the signal band, and equal to $Y_0(f)$ elsewhere:

$$X_1(f) = \tilde{\mathbf{H}}Y_0(f) + (1-\tilde{\mathbf{H}})S_0(f), \tag{4}$$

where $\tilde{\mathbf{H}}=H(f-f_0)-H(f+f_0)$ and H is the Heaviside function. This spectrum is inverse Fourier transformed to the time domain, forming $s_1(t)$. This process us repeated with a new threshold. The updated trace $s_{k+1}(t)$ is given in terms of $s_k(t)$:

$$s_{k+1}(t) = F^{-1}(\tilde{\mathbf{H}}F(\Gamma_k s_k(t)) + (1-\tilde{\mathbf{H}})F(s_k(t))), \tag{5}$$

where F and F^{-1} indicate Fourier and inverse Fourier transforms respectively.

Band-limited impedance inversion

Band-limited impedance inversion (BLIMP) extracts low frequencies from well log data for seismic inversion (Ferguson and Margrave, 1996). To approximate the impedance of the subsurface imaging using seismic data, it is necessary to account for the band-limited nature of the seismic data, especially at low frequencies. The normal incidence reflection coefficient is given as:

$$r_j = \frac{I_{j+1} - I_j}{I_{j+1} + I_j}\ , \tag{6}$$

where r and I indicate reflection coefficient and impedance respectively. Solving equation (6) for I_{j+1}:

$$I_{j+1} = I_1 \prod_{k=1}^{j} \frac{1+r_k}{1-r_k}, \tag{7}$$

Taking the logarithm on both sides of equation (7) and setting: $s_k = \frac{2r_k}{\gamma}$, equation (7) becomes:

$$I_{j+1} = I_1 \mathbf{exp}\left(\gamma \sum_{k=1}^{j} s_k \right). \tag{8}$$

Equation (8) integrates the seismic trace and then exponentiates the result to provide an impedance trance.

Numerical Examples

Figure 1 shows the true Marmousi-II P-wave velocity model. The Marmousi-II model has 244 X 681 grid cells with a grid interval of 10 m in both horizontal and vertical directions. Figure 2a shows the initial model by smoothing the true model with a Gaussian function. As we can see, this initial model contains long wavelength structure. Figures 2b, 2c and 2d show the inversion results with the frequency bands of 1 Hz-30 Hz, 3 Hz-30 Hz and 6 Hz-30 Hz. It can be observed that the velocity model can be reconstructed very well with this initial model, even though the low frequencies are missed.

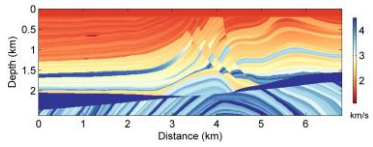

Figure 1. True P-wave velocity model.

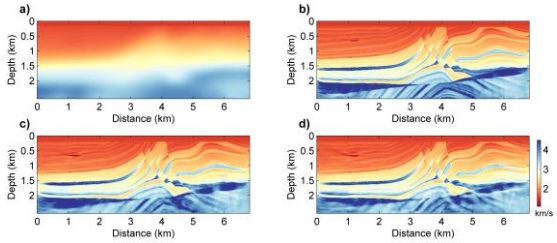

Figure 2. (a) Initial model; (b), (c), and (d) are the inverted models with frequency bands of 1-30 Hz, 3-30 Hz, and 6-30 Hz.

Figure 3a shows the linear initial model, which represents a poor start model for FWI. Figures 3b, 3c and 3d show the inversion results with the frequency bands of 1 Hz-30 Hz, 3 Hz-30 Hz and 6 Hz-30 Hz. We can see that without low frequencies, the model cannot be reconstructed well. Figure 3e shows the model with well log data interpolation. Figure 3f shows the inversion result with well log data regularization and frequency band of 6 Hz-30 Hz. Comparing Figure 3d with 3f, we notice that the well data regularization technique can help to mitigate the cycle-skipping difficulty.

In this research, we suppose a band-limited time reflectivity section can be obtained with traditional seismic data processing flow. Figure 4a shows the frequency spectrum of the time reflectivity section. Figures 4b shows the band-limited time reflectivity section. Figure 4c shows the recoverd frequency spectrum of the reflectivity section with POCS algorithm. A band-limited impedance inversion is then performed with the recovered reflectivity section and the well log data interpolation model. An enhanced initial model is obtained as shown in Figure 5a. Figures 5b, 5c and 5d show the inversion results with the frequency bands of 1-30 Hz, 3-30 Hz and 6-30 Hz. As we can see, comparing Figure 5c with Figure 3c, the inversion result

has been improved obviously. In comparison with Figure 3d, we notice that the inversion result shown in Figure 5d has also been improved.

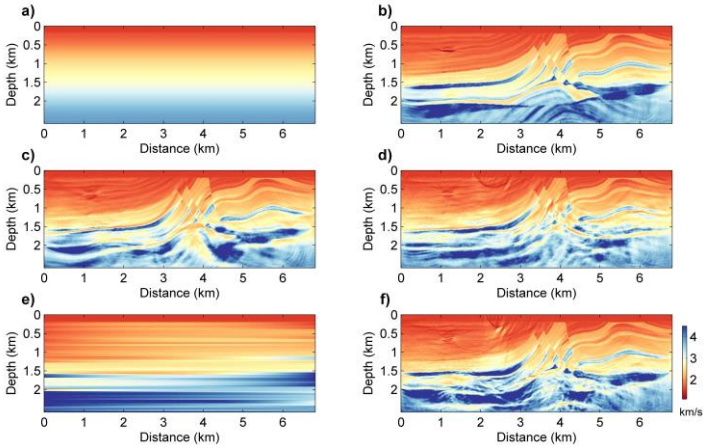

Figure 3. (a) Initial model; (b), (c), and (d) are the inverted models with frequency bands of 1-30 Hz, 3-30 Hz, and 6-30 Hz. (e) is the model by well log data interpolation. (d) is the inversion result with frequency band of 6-30 Hz.

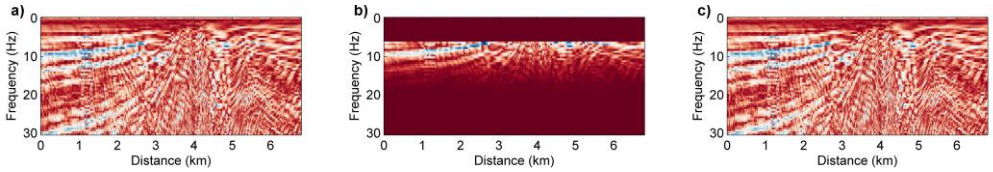

Figure 4. (a) The frequency spectrum of the reflectivity section with full frequency band; (b) the band-limited reflectivity section; (c) The recoverd frequency spectrum with POCS algorithm.

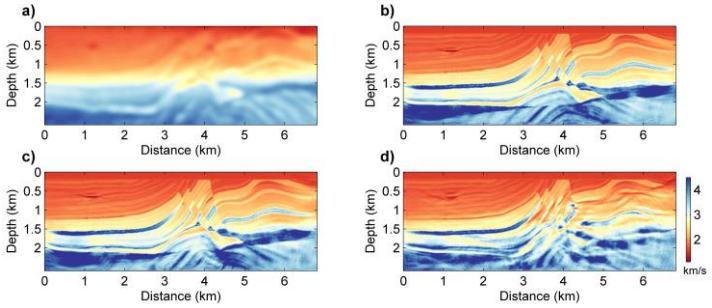

Figure 5. (a) the enhanced initial model; (b), (c) and (d) show the recovered velocity models with frequency bands of 1-30 Hz, 3-30Hz and 6-30 Hz respectively.

Conclusions

In this paper, we are trying to recover low frequencies for full-waveform inversion with band-limited impedance inversion combined with a POCS algorithm. We illustrate with numerical examples that the inversion results can be improved by the proposed strategies.

Acknowledgements

This research was supported by the Consortium for Research in Elastic Wave Exploration Seismology (CREWES) and National Science and Engineering Research Council of Canada (NSERC, CRDPJ 379744-08).

References

Lailly, P., 1983, The seismic inverse problem as a sequence of before stack migration: Conference on Inverse Scattering, Theory and Applications, SIAM, Expanded Abstracts, 206-220.

Ferguson, R. J., and Margrave, G. F., 1996, A simple algorithm for band-limited impedance inversion: CREWES Annual Report, 1–10.

Innanen, K., 2011, A POCS algorithm for spectral extrapolation: CREWES Annual Report, 1–10.

Pratt, R. G., C. Shin, and G. J. Hicks, 1998, Gauss-Newton and full Newton methods in frequency-space seismic waveform inversion: Geophysical Journal International, 133, 341-362.

Pan, W., K. A. Innanen, and G. F. Margrave, 2014a, A comparison of different scaling methods for least-squares migration/inversion: EAGE Expanded Abstracts, We G103 14.

Pan, W., K. A. Innanen, G. F. Margrave, and D. Cao, 2015a, Efficient pseudo-Gauss-Newton full-waveform inversion in the t-p domain: Geophysics, 80, no. 5, R225-R14.

Pan, W., K. A. Innanen, G. F. Margrave, M. C. Fehler, X. Fang, and J. Li, 2015b, Estimation of elastic constants in HTI media using Gauss-Newton and Full-Newton multi-parameter full waveform inversion: SEG Technical Program Expanded Abstracts, 1177-1182.

Pan, W., G. F. Margrave, and K. A. Innanen, 2014b, Iterative modeling migration and inversion (IMMI): Combining full waveform inversion with standard inversion methodology: SEG Technical Program Expanded Abstracts, 938-943.

Tarantola, A., 1984, Inversion of seismic reflection data in the acoustic approximation: Geophysics, 49, 1259-1266.

Virieux, A. and S. Operto, 2009, An overview of full-waveform inversion in exploration geophysics: Geophysics, 74, no. 6, WCC1-WCC26.